ICES Journal of Marine Science, 2023, **80**, 1277–1290
DOI: 10.1093/icesjms/fsad052
Advance access publication date: 3 April 2023
Original Article

Using machine learning to alleviate the allometric effect in otolith shape-based species discrimination: the role of a triplet loss function

Yuwen Chen[1,2] and Guoping Zhu [1,2,3,4,*]

[1]College of Marine Sciences, Shanghai Ocean University, Shanghai 201306, China
[2]Center for Polar Research, Shanghai Ocean University, Shanghai 201306, China
[3]Polar Marine Ecosystem Group, The Key Laboratory of Sustainable Exploitation of Oceanic Fisheries Resources, Ministry of Education, Shanghai 201306, China
[4]National Engineering Research Center for Oceanic Fisheries, Shanghai 201306, China

[*] *Corresponding author: tel: +86 21 6190 0396;* e-mail: gpzhu@shou.edu.cn.

Species identification by fish otoliths is an effective and appropriate approach. However, the allometric growth of otoliths can cause discrimination confusion, particularly in juvenile otolith classification. In the Southern Ocean, *Chionodraco rastrospinosus*, *Krefftichthys anderssoni*, *Electrona carlsbergi*, and *Pleuragramma antarcticum* are frequently caught together in krill fishery as bycatch species. Furthermore, the otolith shape of these four species is relatively similar in juvenile fish, making the identification of fish species difficult. In this study, we tried and evaluated many commonly used machine learning techniques to solve this problem. Eventually, by introducing a triplet loss function (function used to reduce intraspecific variation and increase inter-specific variation), the discrimination confusion caused by the allometric growth of otoliths was reduced. The classification results show that the neural network model with the triplet loss function achieves the best classification accuracy of 96%. The proposed method can help improve otolith classification performance, especially under the context of limited sampling effort, which is of great importance for trophic ecology and the study of fish life history.

Keywords: allometric effect, antarctic, neural network, otolith shape, wavelet transform.

Introduction

Taxonomic studies of marine fish species are important for resource conservation and fishery management if those species are of commercial importance. Therefore, it is necessary to correctly identify species and evaluate their ontogeny and evolutionary relationships (Bani *et al.*, 2013). The techniques used for such studies are often based on conventional shape measurements of body and hard parts, colour patterns, and genetics (Kartika and Herumurti, 2016; Marti-Puig *et al.*, 2020; Bernard *et al.*, 2022). However, molecular and genetic approaches require a lot of time and money. The morphological, structural, and chemical properties of hard parts, especially otoliths, have been used widely for species or population discrimination in the past decades as an effective and suitable tool (e.g. Campana and Neilson, 1985; Campana, 1999; Zhu *et al.*, 2018; Duan *et al.*, 2021; Wei and Zhu, 2022, among others).

Fish have three pairs of otoliths (sagitta, lapillus, and asteriscus) located in different sacs of the inner ear, which are important crystal structures that act as organs of equilibrium and sound transduction (Campana and Casselman, 1993) and are composed of calcium carbonate (98%), organic matrix (2%), and a few other elements (Falini *et al.*, 2005). Among them, the shape of sagittal otoliths is influenced by genetic factors, age, and environmental conditions, especially high morphological variations in genetics (Vignon and Morat, 2010). Furthermore, the otoliths are simple to obtain, and the shape can be efficiently extracted using dedicated software (Lin and Al-Abdulkader, 2019a; Sadighzadeh *et al.*, 2012). Therefore, using otolith to identify fish species has a more distinct and irreplaceable significance in ecology and trophic studies (Lefkaditis *et al.*, 2006), which has been widely recognized and used for the past decades.

Otolith shape is species-specific and often varies allometrically during fish growth (Monteiro *et al.*, 2005; Hussy, 2008; Huang *et al.*, 2021; Wei and Zhu, 2022, among others). This allometric growth brings about intraspecific variation of conspecific otolith (Lychakov and Rebane, 2000). When otolith shape is used as a tool to discriminate fish species, allometric shape changes in otoliths create a discrimination controversy due to these ontogenetic variations could be confused with species variation. Few studies have quantified intraspecific allometric changes in otolith shape or relative dimensions (Monteiro *et al.*, 2005), with many of them so far focusing on S:O ratios (Lombarte, 1992; Aguirre and Lombarte, 1999; Simoneau *et al.*, 2000). Other aspects of allometric shape modification have not been studied in detail, owing to the difficulty in extracting shape information from such a structure with few reference points that can be used as landmarks in the modern toolkit of geometric morphometrics (Bookstein, 1991).

Generally, allometric growth is a negative factor for species identification in otolith taxonomic studies. The key factor is that the allometric effect of the otolith will cause significant intraspecific variation that affects the accuracy of interspecies discrimination (Wong *et al.*, 2016). The tremendous

Received: 27 September 2022; **Revised:** 17 January 2023; **Accepted:** 10 March 2023

Table 1. Sample information.

Species	N	ML (cm)	N0	N1	Sampling period	Min.–Max.	Average ± *SD*
ELC	42	7.6[a]	19	23	2018 Feb	6.0–9.3	7.69 ± 1.18
ANS	41	13.0[b]	17	24	2018 Mar	6.1–20.0	13.33 ± 5.54
KIF	40	30.0[c]	33	7	2016 Mar	11.8–37.9	21.32 ± 6.62
KRA	36	4.8[d]	11	25	2018 Jan	2.2–8.2	5.80 ± 1.38
Total	159						

Size at 50% sexual maturity was introduced to ensure that the selected fish samples have at least two life-history stages (mature and immature). Superscripts indicate references to body length at 50% sexual maturity, where a, b, c, and d are referenced to Mazhirina (1991), La Morales-Nin *et al.* (2000), La Mesa *et al.* (2012), and Koubbi et al. (2003), respectively. *N*, Sample size. ML, Body length at 50% sexual maturity. N0, Immature sample size; N1, Mature sample size. Min. and Max., Minimum and maximum standard length of samples. *SD*, Standard deviation. ELC, *E. carlsbergi*; KIF, *C. rastrospinosus*; ANS, *P. antarcticum*; and KRA, *K. anderssoni*.

inter-specific variation shows that almost only the otoliths of adult fish can be effectively identified (Stock *et al.*, 2021). Unfortunately, to date, few methods have been developed for removing the negative effects of allometric growth when performing otolith shape-based species identification. One of the few approaches is to use analysis of variance to remove shape features significantly correlated with body size (Lombarte and Lleonart, 1993; Tuset *et al.*, 2021). However, the lack of sufficient features to describe the otolith shape may cause difficulties for the classifiers (Simoneau *et al.*, 2000). Another approach is to adjust the values of shape features based on body size using the Lombarte and Lleonart method (1993). These methods are unsatisfactory because it has not treated species specificity in many details. Moreover, no studies have been conducted to verify the effectiveness of this method. To that end, effective species identification based on otolith shape requires a solution that balances inter- and intraspecific differences, which places higher demands on the classifier's recognition ability to discriminate fish species.

In the Southern Ocean, Nototheniids (the main Teleost family in Antarctic waters) is characterized by rapid evolution (Eastman, 1991). The rapid and broad ecological diversification of the family and the knowledge of its molecular phylogeny (Bargelloni *et al.*, 2000; Near *et al.*, 2004) renders it particularly attractive for otolith studies (Lombarte *et al.*, 2010). The Antarctic silverfish *Pleuragramma antarcticum*may be the most abundant fish species in high Antarctic waters, and its ecological significance may rival that of the Antarctic krill *Euphausia superba* —the keystone species in the Southern Ocean (Radtke *et al.*, 1993). Icefishes (family Channichthyidae) are unique among vertebrates because of their lack of hemoglobin. The ocellated icefish *Chionodraco rastrospinosus* is the most common channichthyid, frequently encountered in krill swarms and with some larval nototheniids, which represent their usual prey (Slosarczyk and Rembiszewski, 1982). Lanternfish (family Myctophidae) are the dominant fish within the global mesopelagic fish community in terms of biomass and diversity, including the Southern Ocean (Gjøsaeter and Kawaguchi, 1980). The electron subantarctic *Electrona carlsbergi* and the rhombic lanternfish *Krefftichthys anderssoni* are two of the most abundant species of the Myctophidae family living in the Southern Ocean (Hulley, 1981; McGinnis, 1982; Piatkowski *et al.*, 1994). The abovementioned four species play an important ecological role in the Southern Ocean's open-ocean food web (Barrera-Oro, 2002; Saunders *et al.*, 2015b). Moreover, those species, including *E. superba*, are themselves predators of macrozooplankton, such as copepods, amphipods, and euphausiids (Pakhomov *et al.*, 1996; Williams *et al.*, 2001; Shreeve *et al.*, 2009). Therefore, they are frequently caught in krill fishery as bycatch species (Wei *et al.*, 2017). Moreover, it is urgent to find a solution to identify fish species in the krill fishery because they are frequently in the larval stages, and it is difficult to discriminate them using body shape or other morphological features (Fulford and Allen Rutherford, 2000; Ward *et al.*, 2009). Note that the otolith shape of these four species is relatively similar in juvenile fish, especially *C. rastrospinosus*, *K. anderssoni*, and *P. antarcticum*, which can make the identification of fish species difficult. Recently, Wei and Zhu (2022) discovered that the allometric effect occurs significantly for the otolith shape of *C. rastrospinosus*, and the life-history stages of this species can be identified based on the ontogenetic variation in otolith shape throughout the life in the Bransfield Strait, Antarctic. However, such an allometric effect has potentially eroded the performance for discriminating this species from other *Chionodraco* species (La Mesa *et al.*, 2020). Motivated by these circumstances, this study tested existing classifier models and developed a neural network (NN) approach to find a suitable classifier to relieve the difficulties of the allometric effect on otolith shape-based fish species identification.

Material and methods

Study area and sampling

A total of 159 fish samples were collected in this study (Table 1), of which 36 *K. anderssoni* specimens were collected from the waters around the Kerguelen Islands, East Antarctic, in February 2018, and the remaining fish specimens were collected from licensed Chinese krill trawlers in the Antarctic Peninsula, West Antarctic (Figure 1). As the bycatch species in krill fishery, information on the collection of those samples has been reported to the Commission for the Conservation of Antarctic Marine Living Resources under the protocol of the Scheme of International Scientific Observation. The otoliths of *K. anderssoni* were extracted from the fish specimens on the deck after performing the biometric measurements and stored in the plastic vials. All other fish samples were stored at −20° after collection and subsequently thawed in the laboratory at the Center for Polar Research, Shanghai Ocean University, where standard length (SL; cm) was measured using a vernier caliper, and sagittal otoliths were extracted. Sagittal otoliths were chosen due to their high inter-specific variation and large size, and they are the most commonly used in comparative taxonomy works (Tuset *et al.*, 2006). The extracted sagittal otoliths were washed in ultrapure water for 10 mins before being dried and finally stored in dry centrifuge vials at room temperature.

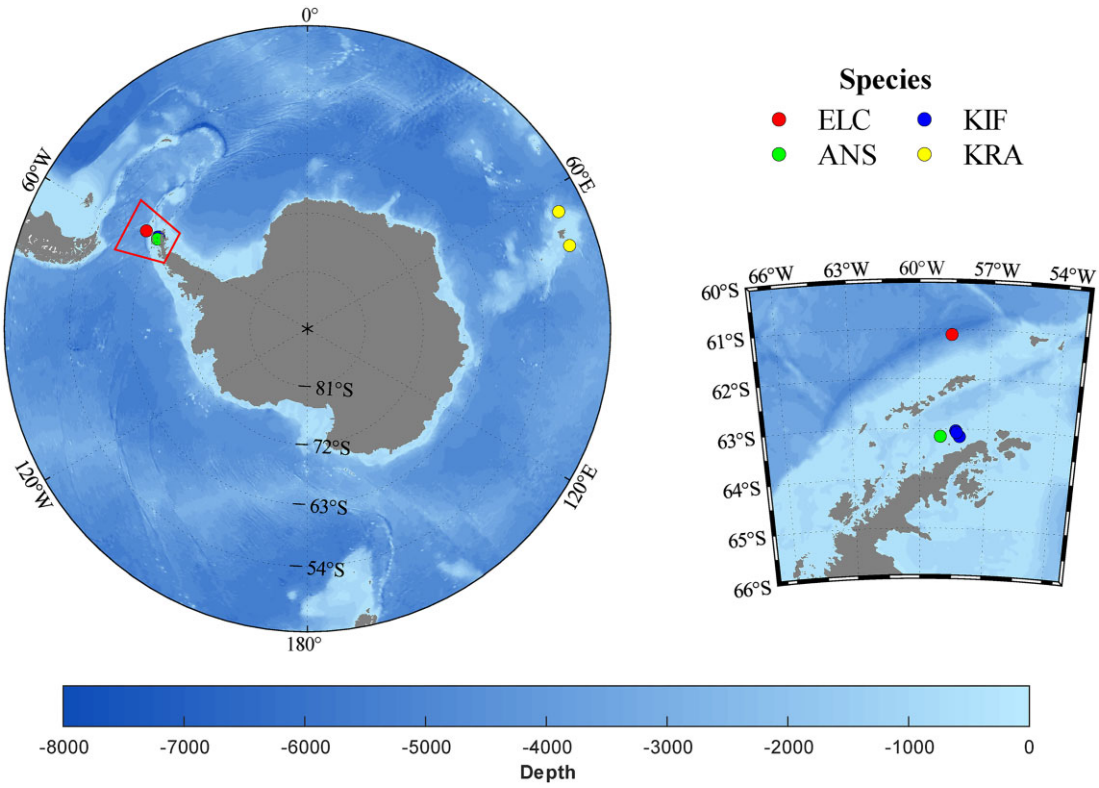

Figure 1. Antarctic and Southern Ocean showing sampling locations and the topography. ELC, *E. carlsbergi*; KIF, *C. rastrospinosus*; ANS, *P. antarcticum*; and KRA, *K. anderssoni*.

The size range of the same fish species was selected as large as possible for the subsequent analysis based on the published studies (La Mazhirina, 1991; Morales-Nin *et al.*, 2000; Koubbi *et al.*, 2003; La Mesa *et al.*, 2012; Lourenço *et al.*, 2017) to ensure that the selected fish samples encompass different life stages of the species (Table 1).

Otolith shape analysis

Extracting otolith outline features requires the acquisition and processing of otolith images. To avoid repetition, the right otolith of fish was selected for further analysis in this study (Volpedo *et al.*, 2008; Saunders *et al.*, 2021). We introduced each step in detail.

For the otolith image acquisition, a microscope (OLYMPUS, SZX7) was used to capture otolith images. Following previous works (Echreshavi *et al.*, 2021), otoliths were placed horizontally with the sulcus toward the bottom against a black background using reflected light. The microscope had an LC30 camera and a PC interface, which allowed for the direct acquisition of high-contrast digital images of otoliths (Figure 2).

For image processing, we read the otolith digital image into R (version 4.0.3; R core team, 2020) and then used the "ShapeR" package for otolith image binarization, otolith contour extraction, contour smoothing, basic otolith measurements, and wavelet analysis (Libungan and Pálsson, 2015).

Based on the scale of the image, ShapeR can be used to acquire four basic measurements of the otolith, namely otolith length (OL, mm), otolith width (OW, mm), otolith perimeter (P, mm), and otolith area (A, mm^2) (Table 2) (Gauldie and Physiology, 1988; Lombarte and Lleonart, 1993; Tuset *et al.*, 2003). The six shape indices of the otolith are then calculated and are shown in Table 3. Next, the otolith length and width are analysed to determine the extent of allometric growth. We used Huxley's allometric equation ($y = ax^b$) to fit the relationship between fish length and otolith length and width (Huxley, 1924). Huxley's allometric equation was estimated with the nonlinear least squares algorithm using the "nls" function in the R program (version 4.0.3, R core team, 2020).

Species classification using statistical classifiers

Twelve statistical classifiers were used to compare their performances in discriminating fish species when experiencing the challenge of the allometric effect. These classifiers are divided into four groups.

1) Classical statistical model classifiers, which include linear discriminant analysis (LDA) (Fisher, 1936), quadratic discriminant analysis (QDA) (Srivastava *et al.*, 2007), and Gaussian Naive Bayesian (GNB) (Wijayanto and Sarno, 2018). LDA and QDA are effective and popular otolith contour discriminant analysis methods, which can achieve better classification results in many cases. GNB is a probabilistic method based on Bayes' theorem.
2) Distance-based classifiers, include nearest centroid classifier machine (NC) (Levner, 2005), K-nearest neighbour algorithms (KNN) (Keller *et al.*, 1985), and radial basis function support vector machine (SVM) (Hearst *et al.*, 1998). Among them, NC has a similar algorithmic idea to the KNN, which is an improvement of KNN and is more efficient than KNN.

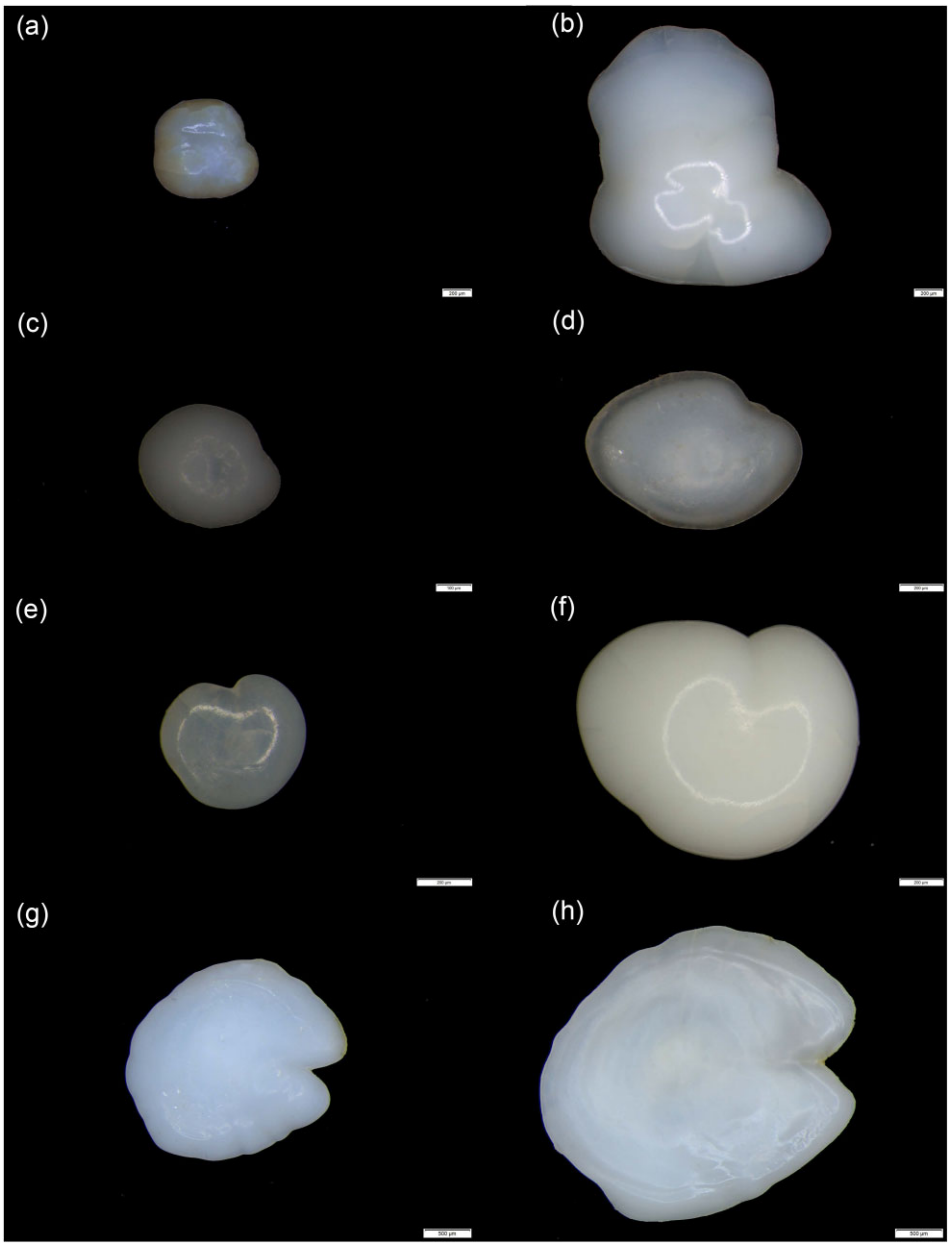

Figure 2. Whole sagittal otoliths of standard length (a) 11.8 cm and (b) 37.9 cm *C. rastrospinosus*, (c) 2.2 cm and (d) 8.2 cm *K. anderssoni*, (e) 6.1 cm and (f) 20.0 cm *P. antarcticum*, (g) 6.0 cm and (h) 9.3 cm *E. carlsbergi*.

Table 2. Shape index formula description.

Shape indices	Formulaic description
Form factor (FF)	$FF = (4 \times \Pi \times A)/P^2$
Rectangularity (R)	$R = A/(OL + OW)$
Elipticity (E)	$E = (OL - OW)/(OL + OW)$
Roundness (r)	$r = (4 \times A)/(\Pi \times OL)^2$
Aspect ratio (AR)	$AR = OL/OW$
Circularity (C)	$C = P^2/A$

OL, Otolith length. OW, Otolith width. P, Otolith perimeter. A, Otolith area.

3) Linear classifiers, include ridge classifier machines (RC) (Peng *et al.*, 2020) and stochastic gradient descent (SGD) (Bottou, 2010). SGD machines allow for the flexible setting of loss functions to solve various classification problems, and RC machines are more capable of dealing with multicollinearity problems than the other linear models.
4) Decision trees (DT) (Safavian *et al.*, 1991), random forest (RF) (Breiman, 2001), gradient boosting classifier machine (GBC) (Friedman, 2001), and AdaBoost classifier machines (ABC) (Solomatine and Shrestha, 2004) are examples of tree structure classifiers. The tree structure algorithm performs well with high-dimensional noisy data. Furthermore, random forests, gradient boosting machines, and AdaBoost machines are all ensemble models that can overcome the shortcomings of weak model generalization ability and achieve better prediction performance.

Wavelet descriptors and shape indices describing the morphology of the otolith are used as an input data in classification. Most studies considered the wavelet function at the fifth

Table 3. Shape index.

Species	FF	R	r	E	C	AR
ELC	0.789 ± 0.017	2.136 ± 0.242	0.276 ± 0.015	0.041 ± 0.031	15.937 ± 0.343	1.089 ± 0.068
ANS	0.811 ± 0.085	2.686 ± 0.952	0.354 ± 0.013	0.058 ± 0.014	15.782 ± 2.876	0.890 ± 0.026
KIF	0.761 ± 0.028	2.309 ± 0.600	0.289 ± 0.035	0.034 ± 0.043	16.335 ± 1.298	1.075 ± 0.098
KRA	0.719 ± 0.194	1.461 ± 0.304	0.255 ± 0.024	0.074 ± 0.074	21.497 ± 16.560	1.169 ± 0.137

FF: Form factor, R: Rectangularity, E: Ellipticity, r: Roundness, AR: Aspect ratio, C: Circularity. ELC, *E. carlsbergi*; KIF, *C. rastrospinosus*; ANS, *P. antarcticum*; and KRA, *K. anderssoni*.

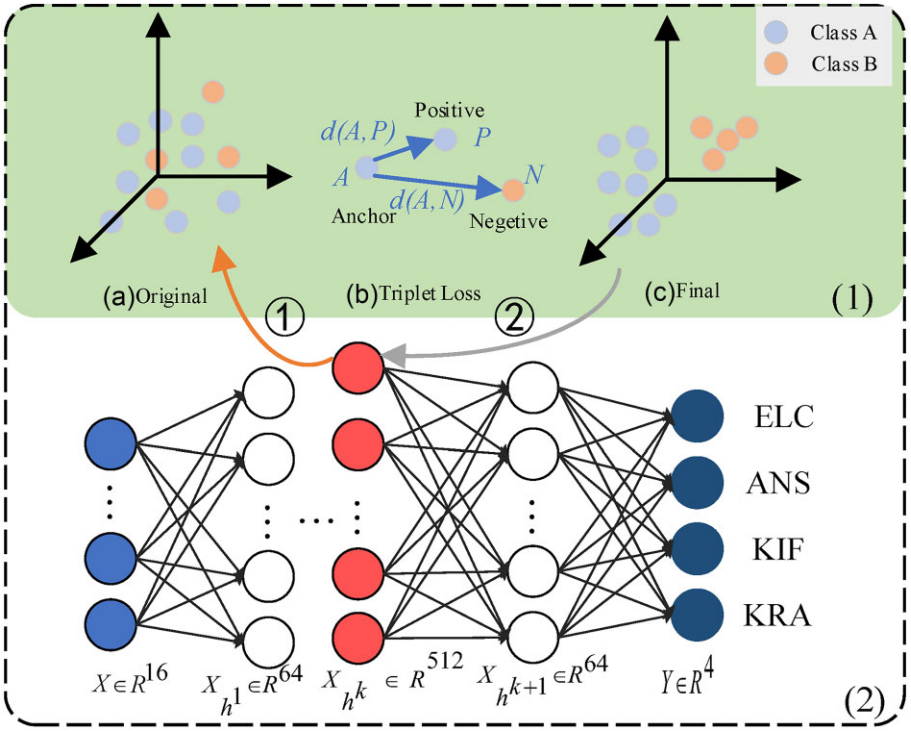

Figure 3. Illustration of the proposed NN structure. We introduced triplt loss (1) in the intermediate layer to reduce the intra-class feature differences of the same fish species and increase the inter-class feature differences of different fish species. ELC, *E. carlsbergi*; KIF, *C. rastrospinosus*; ANS, *P. antarcticum*; and KRA, *K. anderssoni*. The NN design is described in detail in section 2.4 of the main text.

scale when selecting a wavelet harmonic number. However, it has also been shown that the number of harmonics of the wavelet transform used affects the classification model's performance (Lin and Al-Abdulkader, 2019). Therefore, in this study, we tested 5th, 10th, and 20th wavelet descriptors as inputs to the classifier. The best number of wavelet descriptors can then be used in combination with the shape indices as input data to achieve the best classification performance. Furthermore, to unify the order of magnitude between the input data, we normalize the input data between 0 and 1. The data were randomly divided into training and test sets ten times to obtain more reliable results, with the 111 and 48 instances selected as training and test sets, respectively. The classifier performance was evaluated by averaging the results ten times. The framework is shown in the Supplementary Figure S1.

Species classification using NN classification

NNs were first proposed ~80 years before. Inspired by the structure of neurons in the brain and its working principles, the first NN model, the MCP model, was proposed (McCulloch and Pitts, 1943). NN typically consist of an input layer, multiple hidden layers, and an output layer, and the network parameters are generally updated iteratively by calculating the gradient of the loss function. By designing the structure of the hidden layers, activation, and loss functions, the NN can show excellent predictive performance for specific classification problems. Therefore, we want to design an NN that can effectively overcome the mass discrimination of fish species caused by allometric otolith growth in this case.

In general, NN solve image classification problems by taking the image as the input and expecting the NN to learn the image's semantic and low-level feature information. Image classification is aided by the learned discriminative features. However, this requires a very large number of otolith images, otherwise it may lead to a high risk of model overfitting in NN (Hawkins, 2004). Besides, the otolith images contain simple semantic information as well as a large amount of redundant background information. Actually, this redundant information is noisy information for the otolith classification. Therefore, in this study, we feed the extracted features into NN. NN are expected to learn the potential feature relationships and then classify the images. Similar to the statistical classifier, wavelet descriptors and shape indices are used as NN classifier input.

The proposed network structure (neural network with triplet loss, NNT) is shown in Figure 3. It has an input layer, an output layer, and five hidden layers $X_h = \{X_{h^i}, i \in (1, 2, \ldots, 5)\}$. The network is connected through full connection layers and a linear unit activation function (Relu) is used between the five hidden layers.

In addition, we find that the otolith shapes in the images are observed to have large intra-class variation and small inter-class variation, which is challenging for their classification. Towards this end, triplet loss function is introduced to constrain the distance in the features in the NN training. The triple loss was first proposed to solve the face recognition problem in which one identity may have many different face images (Schroff *et al.*, 2015). It was employed to embed input features into feature space such that the squared distance between faces of the same identity is small, while the squared distance between face images from different identities is large (Schroff *et al.*, 2015).

In this study, we mapped the extracted shape features to a high-dimensional feature space through the NN. Next, we used triplet loss to constrain the feature distances between the same species to be small and between different species to be large. The constraint was achieved by introducing a triplet loss function to update the NN parameters through a back propagation algorithm, thereby obtaining the best feature extractor and classifier. Given a set of otolith images $R = \{R_1, R_2, \ldots, R_N\}$, and labels $L = \{L_1, L_2, \ldots, L_n | L_i \in \{A, B\}\}$, as shown in Figure 3, and we first extract features $X = \{X_1, X_2, \ldots, X_n\}$ for each image R_i, where X_i is the input of NNT and $X_i \in \mathbb{R}^{16}$. Triplet loss function then contrains the high-dimensional features $X_{h^k} = \{X^1_{h^k}, X^2_{h^k}, \ldots, X^n_{h^k} | X^i_{h^k} \in \mathbb{R}^{512}\}$ extracted by the $k-th$ hidden layer of the NN. Further, we iteratively sample feature $X^i_{h^k}$ in X_{h^k} as anchor a, and mine $X^j_{h^k}$ as the positive example P corresponding to a and $X^k_{h^k}$ as the negative example N corresponding to a. It is required that $L_i = L_j$ and $L_i \neq L_k$. The constraint objectives are as follows

$$\mathcal{L} = max\left(d\left(a, P\right) - d\left(a, N\right) + margin, 0\right),$$

where $a, P, N \in \mathbb{R}^{512}$. *Margin* indicates the distance of the constraint. $d(a, P)$ indicates the distance between a and P and $d(a, N)$ indicates that between a and N. In this study, the Euclidean distance was introduced

$$d(a, P) = \frac{1}{k}\sum_{i}^{k} \|a_i - P_i\|_2 ,$$

where a_i and P_i indicate each item of a and P, respectively.

The NN is randomly initialized to map the otolith shape features to the feature space. Figure 3(a) shows the original feature space of the shape features after random initialization. Triplet Loss treats Class A as a positive sample and Class B as a negative sample and matches an anchor for the positive sample, as shown in Figure 3(b), and calculates the Euclidean distance between the positive and negative samples and the anchor, respectively. Each sample is selected as an anchor, in which the farthest sample distance of the same class, and the nearest sample distance of different classes are recorded. If the distance between the positive sample and the anchor is less than the margin, then the loss is 0. Otherwise, the loss is the distance between the anchor and positive sample minus the distance between the anchor and negative sample, plus the margin. The triple loss and the cross-entropy loss functions applied to the softmax layer are accumulated as the total loss for the training. Using gradient descent and backward propagation the shape features' mapping is updated, and the total loss are reduced. Finally, the smaller intra-class distances, larger inter-class distances are achieved [Figure 3(c)]. In this study, a triplet loss function is used in X_{h^4} and a cross-entropy loss function (De Boer et al., 2005) is used in the classification layer.

To show the role of the triplet loss function, ablation experiments were designed in this study, with Experiment 1 using only the cross-entropy loss function and Experiment 2 using both the cross-entropy loss function and the triplet loss function, with the same NN settings except for the loss function. To further validate the NN's effectiveness, t-SNE (Van der Maaten and Hinton, 2008) was performed on the test set. The output eigenvalues from the trained NN's fourth hidden layer, where triplet loss is used, were recorded and subjected to t-SNE dimensionality reduction. Default parameter values of the t-SNE algorithm were used, with the number of iterations set to 400.

Our experiments were conducted on a single Nvidia Geforce RTX2060 GPU. The model was implemented using PyTorch (Paszke et al., 2017), an open-source deep learning framework for Python. The epoch is set to 1000, the batch size to 128, the learning rate to 0.001, and the margin to 1.

Table 4. Evaluation metrics.

Evaluation indicators	Formulaic description
Accuracy	$Accuracy = \frac{TP+TN}{TP+FN+FP+TN}$
Precision	$Precision = \frac{TP}{TP+FP}$
Recall	$Recall = \frac{TP}{TP+FN}$
F1-score	$F_1 = \frac{2\times Precision\times Recall}{(Precision+Recall)}$

TP, True positive. TN, True negative. FN, False negative. FP, False positive.

Model evaluation and NN model overfitting test

To better visualize the classification performance of otoliths with varying degrees of allometric growth under different classifiers, we calculate accuracy, recall, precision, and F1-score as metrics of model performance (Table 4). To test the risk of overfitting in the proposed NN, the data were randomly divided into training, validation, and test sets ten times, with the 95, 32, and 32 instances selected as training, validation, and test sets, respectively. In each training, we recorded the training and validation losses. In addition, we calculated the average accuracy of the validation and test sets.

Results

Allometric growth in otolith

The allometric coefficient b differs in the four species (Table 5). The allometric coefficient values of ELC (0.6661) and ANS (0.7216) are closer to 1, compared to KIF (0.5245) and KRA (0.2537), implying a smaller allometric growth. A smaller allometric coefficient value indicates a greater growth rate change. Thus, KIF and KRA have more pronounced allometric growth effects, which would result in more shape variations in otoliths of different body lengths.

Table 5. Result of otolith length and width allometric equation model.

Species	a_1	b_1	RSS_1	a_2	b_2	RSS_2
ELC	1.5537	0.6661	2.656	1.1539	0.7721	3.337
ANS	1.0305	0.7216	49.34	1.0729	0.7518	61.36
KIF	1.2931	0.5245	105.9	1.4810	0.4560	74.4
KRA	2.7619	0.2537	25.31	2.6143	0.1884	15.22

ELC, *E. carlsbergi*; KIF, *C. rastrospinosus*; ANS, *P. antarcticum*; and KRA, *K. anderssoni*. In the table, symbols a_1 and a_2 represent the proportionality coefficients, b_1 and b_2 are allometric coefficients, and RSS_1 and RSS_2 represent the residual sum of squares of otolith length and fish length fitting model and residual sum of squares of otolith width and fish length fitting model, respectively.

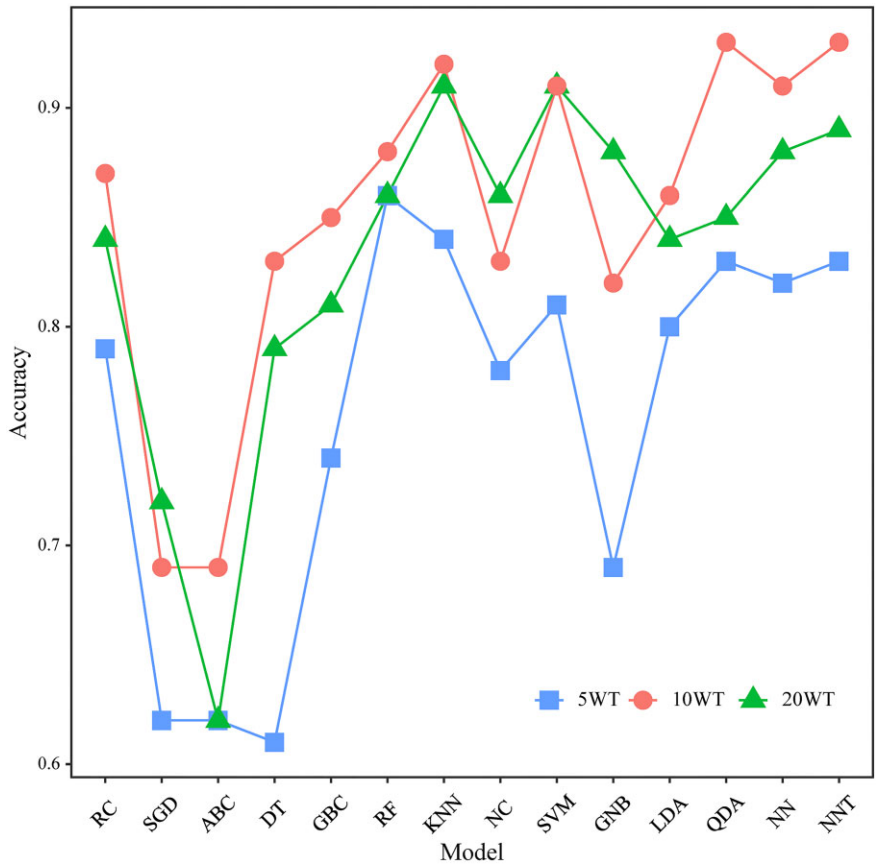

Figure 4. Line graphs of the classification accuracy. 5WT, The first five wavelet harmonics. 10WT, The first ten wavelet harmonics. 20WT, The first 20 wavelet harmonics. ABC, AdaBoost classifier machine. SGD, Stochastic gradient descent machine. SVM, Support vector machine. DT, Decision tree. NC, Nearest centroid classifier machine. RC, Ridge classifier machine. GNB, Gaussian Naive Bayes. KNN, K-nearest neighbour. RF, Random forests. LDA, Linear discriminant analysis. QDA, Quadratic discriminant analysis. GBC, Gradient boosting classifier machine. NN, Neural networks. NNT, Neural networks with triplet loss function.

Variability in otolith shape

To compare the difference in classification performances using the first 5, 10, and 20 wavelet harmonics, the accuracy of 14 classifiers is calculated. The classification accuracy for most classifiers of 10 wavelet harmonics is higher than those of 5 and 20 harmonics (Figure 4). When only the first five wavelet harmonics were used as input data for classification, half of the classifiers obtained classification accuracy below 80%, with the the RF classifier achieving the highest classification accuracy (86%). Similar classification accuracy was achieved by most classifiers using the first 10 vs. 20 wavelet harmonics as input data. In contrast, higher accuracy was always obtained using the first ten wavelet harmonics for tree-based (ABC, DT, GBC, and RF) and NN-structured classifiers. KNN and SVM achieved the highest classification accuracy (91%) using the first 20 wavelet harmonics. Therefore, using the first ten wavelet harmonics is optimal because ten classifiers achieved the highest classification accuracy (mostly between 80 and 90%). Moreover, the highest classification accuracy of 93% was obtained by NNT and QDA, using ten wavelet harmonics as input data. Therefore, 16 features consisting of the first ten wavelet harmonics and shape indices, were selected as input data for the subsequent analysis.

Classification performance

Figure 5 shows the classification performance (accuracy, recall, precision, and F1-score) using the first ten wavelet harmonics and six shape indices for each species. After adding shape indices as input data, all classifiers (except QDA) obtained classification accuracy not lower than those using only ten wavelet harmonics as input data (Figure 5, Sup-

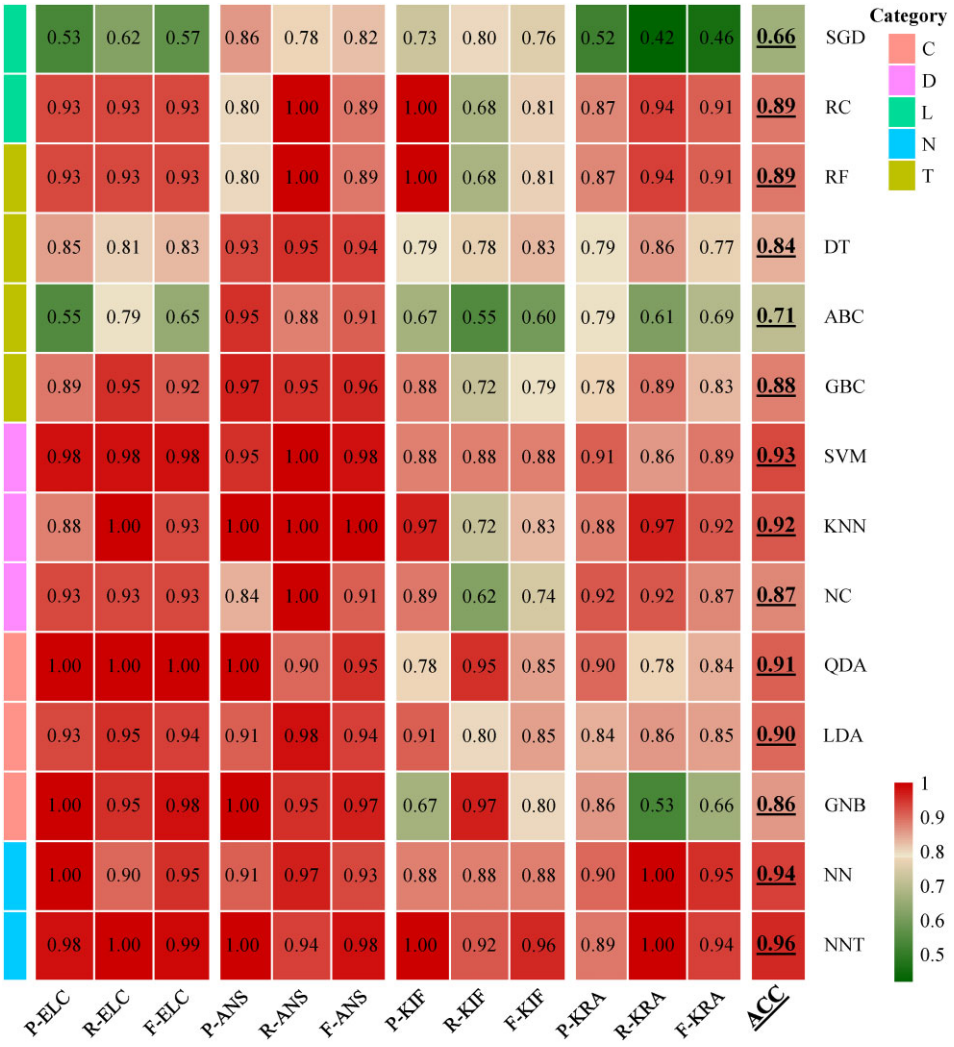

Figure 5. Heatmap of the five categories of classifiers. The horizontal axis represents the performance of the species (ELC, ANS, KRA, and KIF) on the evaluation metrics (P, Precision; R, Recall; F, F1-score), e.g. "P-ELC" represents the precision of ELC. ACC, Classification accuracy, which is underlined to highlight. C, Classical statistical classifier. D, Distance-based classifier. L, Linear classifier. T, Tree classifier. NN, Neural networks classifier. The vertical axis represents the classifiers described in detail in sections 2.3 and 2.4 of the main text.

plementary Table S2). Six classifiers obtained >90% classification accuracy, and NNT obtained the highest classification accuracy (96%). Compared to using the cross-entropy loss function alone, utilizing both the triplet loss and cross-entropy loss functions improves the classification accuracy by 2%.

Considering the classification performance among different species, most classifiers achieved good classification performance for ELC and ANS, the classification precision and recall were mostly above 0.85. F-score, as a composite of precision and recall, is also higher than KIF and KRA in terms of ELC and ANS. The exceptions are ABC and SGD, which have a better classification performance on ANS only, and their classification accuracies were the lowest (0.71 and 0.66, respectively). For most classifiers, KIF and KRA contributed a high proportion of the classification errors. For classification precision, KIF (lowest: 67% and highest: 100%) was higher than KRA (lowest: 52% and highest: 92%). For recall, KRA showed a more variable range (from 42 to 100%), with overall higher values (a total of ten classifiers above 80%) than KIF. Nine classifiers achieved a recall of not >80% for KIF. Generally, ELC and ANS consistently achieved good precision, recall, and F1-score performance. With intense allometric growth, KIF and KRA performed poorly based on the F1-score, the former owing to lower recall and the latter due to lower precision (Figure 5). Figure 5 shows that the strong allometric growth negatively impacts most classifiers.

For the five categories of classification models (Figure 5), the performance of classifiers based on a tree structure is unstable, and among them, performance of the RF algorithm is excellent with an accuracy of 89%. In the linear model-based classifiers, the accuracy of the RC (89%) far exceeds that of the SGD (66%). Overall, classical statistical model-based classifiers, distance-based classifiers, and NN models are suitable for classification. These three categories of classifiers were able to overcome the negative effects of otolith allometric growth to some extent, and the classification accuracy exceeded 85%. In particular, the proposed NN classifier with triplet loss function presents the highest classification accuracy (96%), proving the validity of triplet loss.

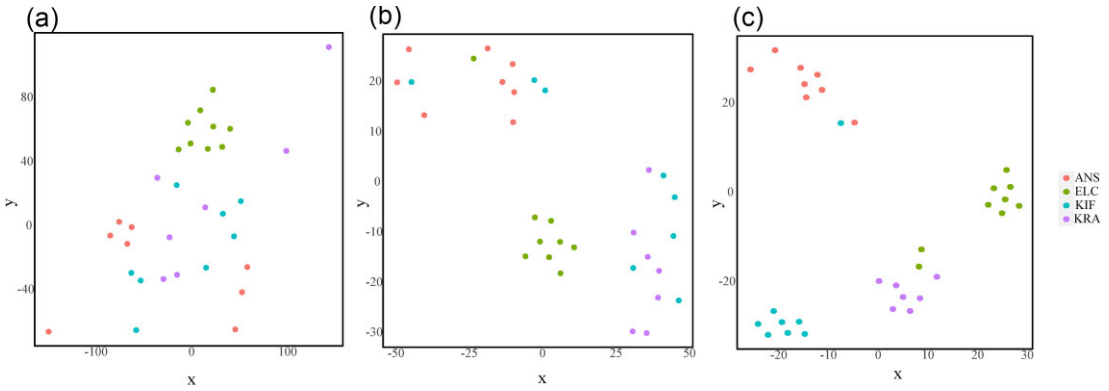

Figure 6. t-SNE visualization using ten wavelet harmonics and six shape indices features on the test set. (a) Original features, (b) fourth layer features for the hidden layer after the NN training, and (c) fourth layer features for the hidden layer after the NN training with triplet loss. ELC, *E. carlsbergi*; KIF, *C. rastrospinosus*; ANS, *P. antarcticum*; and KRA, *K. anderssoni*.

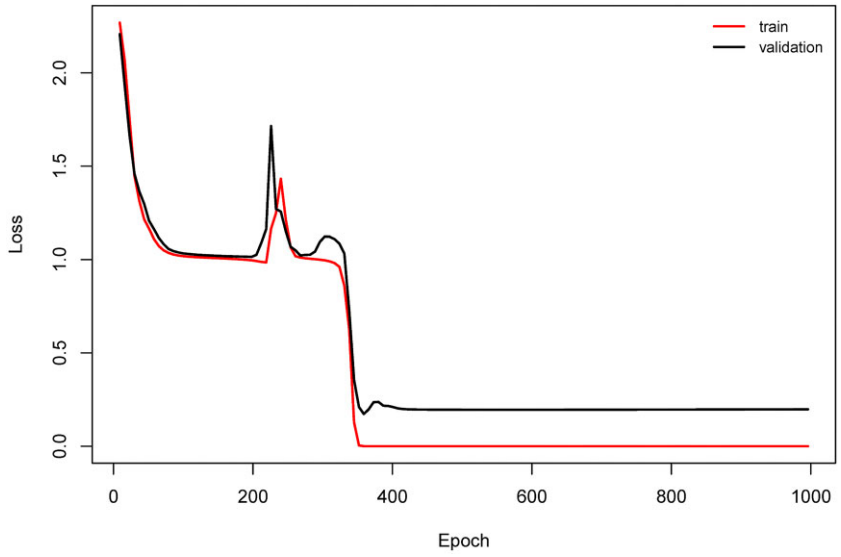

Figure 7. Learning curve plot. Training and validation losses over 1000 epochs during the NN training with triplet loss.

Visualization and overfitting test of the network

T-SNE reduces the dimensionality of the test set by 2. Figure 6 shows the results of (a) t-SNE in the original features, (b) the features trained by the NN, and (c) the features trained by the NNT. The dimensionality reduction of the raw untrained otolith shape features are mixed [Figure 6(a)], especially for KIF, ANS, and KRA. After the NN training, all otoliths can be better divided into three groups, where KIF is confused with KRA and ANS [Figure 6(b)]. In Figure 6(c), the t-SNE plots generated from the data trained by the proposed NN showed the large separation between the four species of fish otoliths, demonstrating the excellent effect of the triplet loss function.

The average accuracy with the ten times random division of the data set for the proposed NN is 0.972 (±0.027) on the validation set and 0.962 (±0.029) on the test set (Supplemenatry Table S1). Similar learning curve is observed in ten times randomized experiments. Take one of them as an example (Figure 7). The learning curves for the training and validation sets show that the NN model did not overfit the data. The plot of training loss decreases to a point of stability. Moreover, the plot of validation loss also decreases to a point of stability and has a small gap with the training loss. However, there is an abrupt jump up and down in the training process due to the learning rate and nature of the gradient descent algorithm.

Discussion

The abovementioned four species (ELC, ANS, KIF, and KRA) play an important ecological role in the Southern Ocean's open-ocean food web (Barrera-Oro, 2002; Saunders *et al.*, 2015c). They provide essential food sources for seabirds, seals, cetaceans, squid, and large predatory fish (Rodhouse *et al.*, 1992; Olsson and North, 1997; Cherel *et al.*, 2002; Collins *et al.*, 2007; Cherel *et al.*, 2008). Therefore, otoliths of these species are vital for studying piscivorous predators' feeding habits. Furthermore, alleviating the problem of species identification caused by otolith allometric growth provides more accurate feeding studies, which contribute significantly to our

understanding of marine food webs, especially at the upper trophic level (Dürr and González, 2002; Garcia–Rodriguez *et al.*, 2011).

In this study, we tested the classification performance of several classifiers in the presence of drastic allometric growth. Our results demonstrated that RF, SVM, and KNN have excellent classification performance despite the negative effect of strong allometric growth. Besides, our study presents an NNT for identifying fish species based on otolith shape while facing the challenge of significant allometric effect. In the ten times randomized experiments, the proposed otolith identification model achieves 0.962 average accuracy on test set. The use of the triplet loss function alleviates the problem of difficult otolith discrimination during the larval period, effectively improving the problem of the low success rate of discrimination of species mixed with otoliths of fish across different life-history stages. The triplet loss can reduce the distance between the intra-group data and widen the inter-group gap data from different groups, allowing a small amount of data to produce the ideal discriminant analysis effect, which is useful for performing otolith-based species identification with a small sample size.

Selection of shape feature

Previous studies always used the first five harmonics of the wavelet transform to describe the otolith shape (Lombarte *et al.*, 2018; Tuset *et al.*, 2018, 2020), but this study discovered that the first five harmonics could achieve certain results but did not achieve the best classification performance. Most classifiers show a saturation result on the number of harmonics after a certain number of harmonics, and increasing the number of harmonics can only slightly improve the classification accuracy in a few cases, such as NC and SGD. Moreover, in most cases, excessively increasing the number of harmonics will result in a lower classification accuracy, especially in tree-based classifiers and NN models (Supplementary Table S2). This may be due to overfitting. Overfitting is one of the fundamental issues in NN, due to continuous gradient updating and scale sensitivity of cross-entropy loss (Salman and Liu, 2019). Tree-based classifier fed with too many variables with insufficient information in training are likely to overfit data (dos Santos *et al.*, 2009). The principle of wavelet transform dictates that the higher the number of harmonics provides more detailed information about the shape (Osowski, 2002), and that part of the information is likely to be redundant in the classification. Among the tree-based models, RF and GBC, the most common ensemble methods, can effectively handle redundant information (Aceña *et al.*, 2022; Moore *et al.*, 2022). Classification performance significantly varies at different numbers of wavelet transform harmonics, suggesting that input features must be chosen more carefully and overfitting must be considered when the sample size is small.

There is significant multicollinearity between shape indices. Moreover, the shape indices are too subjective and causes confusion with certain specific otolith patterns (Tuset *et al.*, 2021). Therefore, using the shape index itself does not achieve satisfactory classification performance. Many studies have shown that using multiple shape feature data provides a more comprehensive description of otolith shape and thus improves the classification performance (e.g. Bourehail *et al.*, 2015; Wong *et al.*, 2016; Avigliano *et al.*, 2018, among others). This phenomenon is observed in most classifiers selected for this study (Supplementary Table S2). With the inclusion of shape indices, >11 classifiers have an accuracy of >85%. The NN model with triplet loss proposed in this study improved the accuracy of otolith classification from 0.93 to 0.96 after incorporating the shape indices. In addition to the NN structure, SVM also shows great potential, and the classification accuracy is improved from 0.91 to 0.93. The great potential of SVM in otolith-based species identification was also reported by Smoliński *et al.* (2020).

Allometric growth and classification performance

The precision, recall, and F1-score of classification result reveals that the allometric growth of otoliths may cause difficulties in otolith-based species classification. The growth of otoliths is more stable and the shape change is not drastic during the whole life-history of ELC and ANS. Good precision and recall are obtained for all classifiers except SGD and ABC. Experimental results show that the ABC and SGD are unsuitable for solving otolith classification problems with strong allometric growth. SGD classifier is rarely used in otolith classification studies. Its poor classification performance is most likely due to setting a large number of hyperparameters requiring heavy parameter tuning (Bottou, 2012). ABC is proved to be relatively stable concerning small training data changes (Ting and Zheng, 2003). However, it is inefficient in classifying otoliths with complex shape variations.

For KIF and KRA, the large allometric growth introduces a large intraspecific variation, resulting in very low precision of classification in most classifiers. Furthermore, the recall of KIF is also very low. These suggest that a portion of KIF otoliths are misclassified as KRA. This misclassification may be due to the high similarity of otoliths between KIF and KRA during juvenile stage. Despite intense allometric growth bringing greater classification difficulty, there are still many classifiers that have been shown to have learned effective classification features. In the tree-based classifiers, both RF and GBC have better classification results. This is because they increase precision at the cost of reducing recall. KNN and RC behave similarly to achieve excellent classification performance. SVM, LDA, and QDA are commonly used classifiers in otolith classification studies and show extraordinary classification performance in many studies. In this study, they demonstrated excellent classification performance despite the negative effect of strong allometric growth. The three classifiers balance precision and recall better and make more reliable predictions. In particular, the SVM classifier achieved an accuracy (93%) second only to the NN classifier. SVMs are widely used in computational biology due to their high accuracy and flexibility in modeling diverse data sources (Schölkopf *et al.*, 2004; Müller *et al.*, 2018). They allow the use of kernels to generate nonlinear decision boundaries. The domain knowledge inherent in any classification task is captured by defining a suitable kernel (Ben-Hur *et al.*, 2008). This study used a nonlinear RBF kernel to achieve a high classification performance. It is somewhat surprising that the top four highest classification accuracies were achieved with the nonlinear classifiers (NNT, NN, SVM, and KNN). Hence, it could conceivably be hypothesized that nonlinear classifiers are robust to classification difficulties caused by the allometric growth of otoliths. It is noteworthy that GBC and RC were rarely used in previous studies, but they produced superior classification results. This gives machine learning models more options for subsequent

studies. RC, in particular, overcomes the negative effects of severe multicollinearity in the otolith shape indices (Lieberman and Morris, 2014; Duzan and Shariff, 2015). However, its potential has received little attention in previous studies.

NN are classification algorithms characterized by flexibility, allowing for designing the network's structure and selecting the appropriate loss function based on the actual situation. Therefore, NN classifiers can achieve satisfactory classification performance in most cases (Soom *et al.*, 2022). However, one of the common issues with deep learning methods is that they are extremely data-intensive. NNs usually require a large amount of data to make useful predictions due to numerous learnable parameters. A lack of data may lead to a mismatch between the order of magnitude of the training set and model complexity, resulting in a high risk of overfitting (Hawkins, 2004). The issue can be considered as one of the bottlenecks in small applications, limiting the development of deep learning in life sciences. We approach this problem in two ways. The first is to combine traditional feature extraction with deep learning models to remove redundant information and extract useful information from otolith's contour. Feature extraction reduces the complexity of the model, avoids the risk of overfitting, and achieves excellent classification performance. The second approach is to introduce the triplet loss to embed the extracted shape features into a feature space, such that intra-class separation is minimized and inter-class separation is maximized. Similarly, triplet loss has been used in many classification applications (e.g. bioacoustic classification, classification of remote sensing scene, and face recognition) (Yeung *et al.*, 2017; Clementino and Colonna, 2020; Zhang *et al.*, 2020). It has been demonstrated to reduce the required sample size by the NN (Thakur *et al.*, 2019).

In future studies, the use of the triplet loss may be considered more often in cases where large intra-class differences affect the inter-class discriminant analysis. More work can be conducted to train the model on otoliths from different fish species at different life-history stages to validate the effectiveness of NN with triplet loss functions.

Acknowledgements

We are grateful to the owners and captains of large-scale trawlers *Furonghai* and *Longteng*, and the scientific observers onboard those vessels for fish sampling and processing. The otoliths from *Kreffticbthys anderssoni* come from the French REPCCOAI surveys (Response of the Pelagic Ecosystem to Climate Change in the Southern Ocean and South Indian). Professor Philippe Koubbi (Sorbonne Université-France) was the PI of the fish project. The REPCCOAI surveys were supported by the French National Fleet and logistically by IFREMER. Team members of the Polar Marine Ecosystem Laboratory, Shanghai Ocean University deserve special recognition for their efforts in the laboratory. We also thank the College of Marine Sciences at Shanghai Ocean University for providing the facilities in the laboratory that made this study happen. Finally, we thank the reviewers who improved the quality of this manuscript.

Supplementary data

Supplementary material is available at the *ICESJMS* online version of the manuscript.

Conflict of interest

The authors declare that they have no conflict of interest.

Author contributions

YWC conducted the lab work, analysed the data, and wrote the manuscript. GPZ designed the concept, supervised the lab work, analysed the data with assistance from YWC and wrote the manuscript. All authors contributed to manuscript writing.

Funding

Funding was provided by the Promote scientific research cooperation and high-level talent training projects with Canada, Australia, New Zealand, and Latin America of Chinese Scholarship Council (grant number 2021-109 to GPZ), the National Science Foundation of China (grant no. 41776185 to GPZ), and the National Key R&D Program of China (grant no. 2018YFC1406801 to GPZ).

Data availability

The datasets created during and/or analysed during the current study are available from the corresponding author upon reasonable request.

References

Aceña, V., de Diego, I. M., Fernández, R. R., and Moguerza, J. M. 2022. Minimally overfitted learners: a general framework for ensemble learning. Knowledge-Based Systems, 254: 109669.

Aguirre, H., and Lombarte, A. 1999. Ecomorphological comparisons of sagittae in *Mullus barbatus* and *M. surmuletus*. Journal of Fish Biology, 55: 105–114.

Avigliano, E., Rolón, M. E., Rosso, J. J., Mabragaña, E., and Volpedo, A. V. 2018. Using otolith morphometry for the identification of three sympatric and morphologically similar species of *Astyanax* from the Atlantic Rain Forest (Argentina). Environmental Biology of Fishes, 101: 1319–1328.

Bani, A., Poursaeid, S., and Tuset, V. M. 2013. Comparative morphology of the sagittal otolith in three species of South Caspian gobies. Journal of Fish Biology, 82: 1321–1332.

Bargelloni, L., Marcato, S., Zane, L., and Patarnello, T. 2000. Mitochondrial phylogeny of notothenioids: a molecular approach to Antarctic fish evolution and biogeography. Systematic Biology, 49: 114–129.

Barrera-Oro, E. 2002. The role of fish in the Antarctic marine food web: differences between inshore and offshore waters in the southern Scotia Arc and west Antarctic Peninsula. Antarctic Science, 14: 293–309.

Ben-Hur, A., Ong, C. S., Sonnenburg, S., Schölkopf, B., and Rätsch, G. 2008. Support vector machines and kernels for computational biology. PLoS Computational Biology, 4: e1000173.

Bernard, A. M., Finnegan, K. A., Sutton, T. T., Eytan, R. I., Weber, M. D., and Shivji, M. S. 2022. Population genomic dynamics of mesopelagic lanternfishes *Diaphus dumerilii*, *Lepidophanes guentheri*, and *Ceratoscopelus warmingii* (Family: Myctophidae) in the Gulf of Mexico. Deep Sea Research Part I: Oceanographic Research Papers, 185: 103786.

Bookstein, F. L. 1991. Morphometric tools for landmark data. In Geometry and Biology. Cambridge University Press, New York. 435 pp.

Bottou, L. 2010. Large-scale machine learning with stochastic gradient descent. In Proceedings of COMPSTAT'2010, pp. 177–186. Ed by Y. Lechevallier, andSaporta G . Physica-Verlag HD, Hiedelberg, Germany.

Bottou, L. 2012. Stochastic gradient descent tricks. In Neural Networks: Tricks of the Trade, pp. 421–436. Ed by Montavon G., Orr G. B., and Müller K. R.. Springer, Berlin, Heidelberg.
Bourehail, N., Morat, F., Lecomte-Finiger, R., and Kara, M. H. 2015. Using otolith shape analysis to distinguish barracudas *Sphyraena sphyraena* and *Sphyraena viridensis* from the Algerian coast. Cybium, 39: 271–278.
Breiman, L. 2001. Random forests. Machine Learning, 45: 5–32.
Campana, S. E. 1999. Chemistry and composition of fish otoliths: pathways, mechanisms and applications. Marine Ecology Progress Series, 188: 263–297.
Campana, S. E., and Casselman, J. M. 1993. Stock discrimination using otolith shape analysis. Canadian Journal of Fisheries and Aquatic Sciences, 50: 1062–1083.
Campana, S. E., and Neilson, J. D. 1985. Microstructure of fish otoliths. Canadian Journal of Fisheries and Aquatic Sciences, 42: 1014–1032.
Cherel, Y., Ducatez, S., Fontaine, C., Richard, P., and Guinet, C. 2008. Stable isotopes reveal the trophic position and mesopelagic fish diet of female southern elephant seals breeding on the Kerguelen Islands. Marine Ecology Progress Series, 370: 239–247.
Cherel, Y., Pütz, K., and Hobson, K. A. 2002. Summer diet of king penguins (*Aptenodytes patagonicus*) at the Falkland Islands, southern Atlantic Ocean. Polar Biology, 25: 898–906.
Clementino, T., and Colonna, J. 2020. Using triplet loss for bird species recognition on BirdCLEF 2020. In: CLEF working notes 2020. L. Cappellato, C. Eickhoff, N. Ferro, and A. Névéol CLEF: Conference and Labs of the Evaluation Forum, Thessaloniki, Greece.
Collins, M. A., Ross, K. A., Belchier, M., and Reid, K. 2007. Distribution and diet of juvenile Patagonian toothfish on the South Georgia and Shag Rocks shelves (Southern Ocean). Marine Biology, 152: 135–147.
De Boer, P. T., Kroese, D. P., Mannor, S., and Rubinstein, R. Y. 2005. A tutorial on the cross-entropy method. Annals of Operations Research, 134: 19–67.
dos Santos, M. E., Sabourin, R., and Maupin, P. 2009. Overfitting cautious selection of classifier ensembles with genetic algorithms. Information Fusion, 10: 150–162.
Duan, M., Ashford, J. R., Bestley, S., Wei, X. Y., Walters, A., and Zhu, G. P. 2021. Otolith chemistry of *Electrona antarctica* suggests a potential population marker distinguishing the southern Kerguelen Plateau from the eastward-flowing Antarctic Circumpolar Current. Limnology and Oceanography, 66: 405–421.
Dürr, J., and González, J. A. 2002. Feeding habits of *Beryx splendens* and *Beryx decadactylus* (Berycidae) off the Canary Islands. Fisheries Research, 54: 363–374.
Duzan, H., and Shariff, N. S. B. M. 2015. Ridge regression for solving the multicollinearity problem: review of methods and models. Journal of Applied Sciences, 15: 392–404.
Eastman, J. T. 1991. Evolution and diversification of Antarctic notothenioid fishes. American Zoologist, 31: 93–110.
Echreshavi, S., Esmaeili, H. R., Teimori, A., and Safaie, M. 2021. Otolith morphology: a hidden tool in the taxonomic study of goatfishes (Teleostei: Perciformes: Mullidae). Zoological Studies, 60: 36.
Falini, G., Fermani, S., Vanzo, S., Miletic, M., and Zaffino, G. 2005. Influence on the formation of aragonite or vaterite by otolith macromolecules. European Journal of Inorganic Chemistry, 2005: 162–167.
Fisher, R. A. 1936. The use of multiple measurements in taxonomic problems. Annals of Eugenics, 7: 179–188.
Friedman, J. H. 2001. Greedy function approximation: a gradient boosting machine. The Annals of Statistics, 29: 1189–1232.
Fulford, R. S., and Allen Rutherford, D. 2000. Discrimination of larval Morone geometric shape differences with landmark-based morphometrics. Copeia, 2000: 965–972.
Garcia-Rodriguez, F. J., De, La, and Cruz-Agüero, J. 2011. A comparison of indexes for prey importance inferred from otoliths and cephalopod beaks recovered from pinniped scats. Journal of Fisheries and Aquatic Science, 6: 186.
Gauldie, R. W. 1988. Function, form and time-keeping properties of fish otoliths. Comparative Biochemistry and Physiology Part A: Physiology, 91: 395–402.
Gjøsæter, J., Gjøsæter, J., and Kawaguchi, K. 1980. A Review of the World Resources of Mesopelagic Fish. Food and Agriculture Organization of the United Nations, Rome. 151pp.
Hawkins, D. M. 2004. The problem of overfitting. Journal of Chemical Information and Computer Sciences, 44: 1–12.
Hearst, M. A., Dumais, S. T., Osuna, E., Platt, J., and Scholkopf, B. 1998. Support vector machines. IEEE Intelligent Systems and their Applications, 13: 18–28.
Huang, Y. F., Song, B. L., Deng, T. H., Wang, Q., Shen, Q., and Liu, L. G. 2021. Ontogenetic development, allometric growth patterns, and daily increment validation of larvae and juvenile *Culter alburnus*. Environmental Biology of Fishes, 104: 1593–1610.
Hulley, P. A. 1981. Results of the research cruises of FRV "Walther Herwig" to South America. LVIII. Family Myctophidae (Osteichthyes, Myctophiformes). Journal of Applied Ichthyology, 26: 32–40.
Hüssy, K. 2008. Otolith shape in juvenile cod (*Gadus morhua*): ontogenetic and environmental effects. Journal of Experimental Marine Biology and Ecology, 364: 35–41.
Huxley, J. S. 1924. Constant differential growth-ratios and their significance. Nature 14: 896–897.
Kartika, D. S. Y., and Herumurti, D. 2016. Koi fish classification based on HSV color space. In 2016 International Conference on Information & Communication Technology and Systems (ICTS), pp. 96–100. IEEE.
Keller, J. M., Gray, M. R., and Givens, J. A. 1985. A fuzzy k-nearest neighbor algorithm. IEEE transactions on systems, man, and cybernetics, SMC-15: 580–585.
Koubbi, P., Duhamel, G., Harlay, X., Eastwood, P., Durand, I., and Park, Y-H. 2003. Distribution of larval *Krefftichthys anderssoni* (Myctophidae, Pisces) at the Kerguelen Archipelago (Southern Indian Ocean) modelled using GIS and habitat suitability. Antarctic Biology in a Global Context: Proceedings of the VIIIth SCAR International Biology Symposium, 2001, Vrije Universiteit, Amsterdam, The Netherlands. Backhuys Publishers. 215–223.
La Mesa, M., and Eastman, J. T. 2012. Antarctic silverfish: life strategies of a key species in the high-Antarctic ecosystem. Fish and Fisheries, 13: 241–266.
La Mesa, M., Guicciardi, S., Donato, F., Riginella, E., Schiavon, L., and Papetti, C. 2020. Comparative analysis of otolith morphology in icefishes (Channichthyidae) applying different statistical classification methods. Fisheries Research, 230: 105668.
Lefkaditis, D., Awcock, G. J., and Howlett, R. J. 2006. Intelligent optical otolith classification for species recognition of bony fish. In International Conference on Knowledge-Based and Intelligent Information and Engineering Systems, pp. 1226–1233. Springer, Berlin, Heidelberg.
Levner, I. 2005. Feature selection and nearest centroid classification for protein mass spectrometry. BMC Bioinformatics [Electronic Resource], 6 1–14.
Libungan, L. A., and Pálsson, S. 2015. ShapeR: an R package to study otolith shape variation among fish populations. PLoS One, 10: e0121102.
Lieberman, M. G., and Morris, J. D. 2014. The precise effect of multicollinearity on classification prediction. Multiple Linear Regression Viewpoints, 40: 5–10.
Lin, Y.-J., and Al-Abdulkader, K. 2019. Identification of fish families and species from the western Arabian Gulf by otolith shape analysis and factors affecting the identification process. Marine and Freshwater Research, 70: 1818–1827.
Lombarte, A. 1992. Changes in otolith area: sensory area ratio with body size and depth. Environmental Biology of Fishes, 33: 405–410.
Lombarte, A., and Lleonart, J. 1993. Otolith size changes related with body growth, habitat depth and temperature. Environmental biology of fishes, 37: 297–306.

Lombarte, A., Miletić, M., Kovačić, M., Otero-Ferrer, J. L., and Tuset, V. M. 2018. Identifying sagittal otoliths of Mediterranean Sea gobies: variability among phylogenetic lineages. Journal of Fish Biology, 92: 1768–1787.

Lombarte, A., Palmer, M., Matallanas, J., Gómez-Zurita, J., and Morales-Nin, B. 2010. Ecomorphological trends and phylogenetic inertia of otolith sagittae in Nototheniidae. Environmental Biology of Fishes, 89: 607–618.

Lourenço, S., Saunders, R. A., Collins, M., Shreeve, R., Assis, C. A., Belchier, M., Watkins, J. L. *et al.* 2017. Life cycle, distribution and trophodynamics of the lanternfish *Krefftichthys anderssoni* (Lönnberg, 1905) in the Scotia Sea. Polar Biology, 40: 1229–1245.

Lychakov, D. V., and Rebane, Y. T. 2000. Otolith regularities. Hearing Research, 143: 83–102.

Marti-Puig, P., Manjabacas, A., and Lombarte, A. 2020. Automatic classification of morphologically similar fish species using their head contours. Applied Sciences, 10: 3408.

Mazhirina, G. 1991. Reproduction of *Electrona carlsbergi* tanning. In Proceedings of the Meeting of the Scientific and Working Group of CCAMLR, pp. 397–409. CCAMLR, Hobart.

McCulloch, W. S., and Pitts, W. 1943. A logical calculus of the ideas immanent in nervous activity. The Bulletin of Mathematical Biophysics, 5: 115–133.

McGinnis, R. F. 1982. Biogeography of Lanternfishes (Myctophidae) South of 30°S. Amercian Geophysical Union, Washington DC. 110pp.

Monteiro, L. R., Di Beneditto, A. P. M., Guillermo, L. H., and Rivera, L. A. 2005. Allometric changes and shape differentiation of sagitta otoliths in sciaenid fishes. Fisheries Research, 74: 288–299.

Moore, B. R., Parker, S. J., and Pinkerton, M. H. 2022. Otolith shape as a tool for species identification of the grenadiers *Macrourus caml* and *M. whitsoni*. Fisheries Research, 253: 106370.

Morales-Nin, B., Moranta, J., and Balguerias, E. 2000. Growth and age validation in high-Antarctic fish. Polar Biology, 23: 626–634.

Müller, K. R., Mika, S., Tsuda, K., and Schölkopf, K. 2018. An introduction to kernel-based learning algorithms. In: Handbook of Neural Network Signal Processing, pp. 4–1. CRC Press, Boca Raton, FL.

Near, T. J., Pesavento, J. J., and Cheng, C. H. C. 2004. Phylogenetic investigations of Antarctic notothenioid fishes (Perciformes: Notothenioidei) using complete gene sequences of the mitochondrial encoded 16S rRNA. Molecular phylogenetics and evolution, 32: 881–891.

Olsson, O., and NORTH, A. W. 1997. Diet of the king penguin *Aptenodytes patagonicus* during three summers at South Georgia. Ibis, 139: 504–512.

Osowski, S. 2002. Fourier and wavelet descriptors for shape recognition using neural networks—a comparative study. Pattern Recognition, 35: 1949–1957.

Pakhomov, E. A., Perissinotto, R., and McQuaid, C. D. 1996. Prey composition and daily rations of myctophid fishes in the Southern Ocean. Marine Ecology Progress Series, 134: 1–14.

Paszke, A., Gross, S., Chintala, S., Chanan, G., Yang, E., DeVito, Z., Lin, Z. *et al.* 2017. Automatic differentiation in pytorch. in 31st Conference on Neural Information Processing Systems (NIPS 2017), pp. 1–4.

Peng, C., and Cheng, Q. 2020. Discriminative ridge machine: a classifier for high-dimensional data or imbalanced data. IEEE Transactions on Neural Networks and Learning Systems, 32: 2595–2609.

Piatkowski, U., and Hagen, W. 1994. Distribution and lipid composition of early life stages of the cranchiid squid *Galiteuthis glacialis* (Chun) in the Weddell Sea, Antarctic Science, 6: 235–239.

Radtke, R. L., Hubold, G., Folsom, S. D., and Lenz, P. H. 1993. Otolith structural and chemical analyses: the key to resolving age and growth of the Antarctic silverfish, *Pleuragramma antarcticum*. Antarctic Science, 5: 51–62.

Rodhouse, P. G., White, M. G., and Jones, M. R. R. 1992. Trophic relations of the cephalopod *Martialia hyadesi* (Teuthoidea: Ommastrephidae) at the Antarctic Polar Front, Scotia Sea. Marine Biology, 114: 415–421.

Sadighzadeh, Z., Tuset, V. M., Valinassab, T., Dadpour, M. R., and Lombarte, A. 2012. Comparison of different otolith shape descriptors and morphometrics for the identification of closely related species of *Lutjanus* spp. from the Persian Gulf. Marine Biology Research, 8: 802–814.

Safavian, S. R., and Landgrebe, D. 1991. A survey of decision tree classifier methodology. IEEE Transactions on Systems, Man, and Cybernetics, 21: 660–674.

Salman, S., and Liu, X. 2019. Overfitting mechanism and avoidance in deep neural networks. arXiv:1901.06566.

Saunders, B., Kitzinger, J., and Kitzinger, C. 2015. Anonymising interview data: challenges and compromise in practice. Qualitative research, 15: 616–632.

Saunders, R. A., Lourenço, S., Vieira, R. P., Collins, M. A., and Xavier, J. C. 2021. Length–weight and otolith size to standard length relationships in 12 species of Southern Ocean Myctophidae: a tool for predator diet studies. Journal of Applied Ichthyology, 37: 140–144.

Schölkopf, B., Tsuda, K., and Vert, J. P. 2004. Kernel Methods in Computational Biology. MIT Press, Cambridge, MA. 140pp.

Schroff, F., Kalenichenko, D., and Philbin, J. 2015. Facenet: a unified embedding for face recognition and clustering. In Proceedings of the IEEE conference on computer vision and pattern recognition, pp. 815–823.

Shreeve, R. S., Collins, M. A., Tarling, G. A., Main, C. E., Ward, P., and Johnston, N. M. 2009. Feeding ecology of myctophid fishes in the northern Scotia Sea. Marine Ecology Progress Series, 386: 221–236.

Simoneau, M., Casselman, J. M., and Fortin, R. 2000. Determining the effect of negative allometry (length/height relationship) on variation in otolith shape in lake trout (*Salvelinus namaycush*), using Fourier-series analysis. Canadian Journal of Zoology, 78: 1597–1603.

Slósarczyk, W., and Rembiszewski, J. M. 1982. The occurence of juvenile Notothenioidei (*Pisces*) within krill concentrations in the region of the Bransfield Strait and the southern Drake Passage. Polish Polar Research, 3: 299–312.

Smoliński, S., Schade, F. M., and Berg, F. 2020. Assessing the performance of statistical classifiers to discriminate fish stocks using Fourier analysis of otolith shape. Canadian Journal of Fisheries and Aquatic Sciences, 77: 674–683.

Solomatine, D. P., and Shrestha, D. L. 2004. AdaBoost. RT: a boosting algorithm for regression problems. In 2004 IEEE International Joint Conference on Neural Networks (IEEE Cat. No. 04CH37541), pp. 1163–1168.

Soom, J., Pattanaik, V., Leier, M., and Tuhtan, J. A. 2022. Environmentally adaptive fish or no-fish classification for river video fish counters using high-performance desktop and embedded hardware. Ecological Informatics, 72, 101817.

Srivastava, S., Gupta, M. R., and Frigyik, B. A. 2007. Bayesian quadratic discriminant analysis. Journal of Machine Learning Research, 8: 1277–1305.

Stock, M., Nguyen, B., Courtens, W., Verstraete, H., Stienen, E., and De Baets, B. 2021. Otolith identification using a deep hierarchical classification model. Computers and Electronics in Agriculture, 180: 105883.

Team, R Core. 2020. R: A language and environment for statistical computing. R Foundation for Statistical Computing, Vienna, Austria. https://www.R project.org/.

Thakur, A., Thapar, D., Rajan, P., and Nigam, A. 2019. Deep metric learning for bioacoustic classification: overcoming training data scarcity using dynamic triplet loss. The Journal of the Acoustical Society of America, 146: 534–547.

Ting, K. M., and Zheng, Z. 2003. A study of adaboost with naive bayesian classifiers: weakness and improvement. Computational Intelligence, 19: 186–200.

Tuset, V. M., Lombarte, A., Bariche, M., Maynou, F., and Azzurro, E. 2020. Otolith morphological divergences of successful Lessepsian

fishes on the Mediterranean coastal waters. Estuarine, Coastal and Shelf Science 236: 106631.

Tuset, V. M., Lozano, I. J., Gonzalez, J. A., Pertusa, J. F., and Garcia-Diaz, M. M. 2003. Shape indices to identify regional differences in otolith morphology of comber, *Serranus cabrilla* (L., 1758). Journal of Applied Ichthyology, 19: 88–93.

Tuset, V. M., Olivar, M. P., Otero-Ferrer, J. L., López-Pérez, C., Hulley, P. A., and Lombarte, A. 2018. Morpho-functional diversity in *Diaphus* spp. (Pisces: Myctophidae) from the central Atlantic Ocean: ecological and evolutionary implications. Deep Sea Research Part I: Oceanographic Research Papers, 138: 46–59.

Tuset, V. M., Otero-Ferrer, J. L., Siliprandi, C., Manjabacas, A., Marti-Puig, P., and Lombarte, A. 2021. Paradox of otolith shape indices: routine but overestimated use. Canadian Journal of Fisheries and Aquatic Sciences, 78: 681–692.

Tuset, V. M., Rosin, P. L., and Lombarte, A. 2006. Sagittal otolith shape used in the identification of fishes of the genus *Serranus*. Fisheries Research, 81: 316–325.

Van der Maaten, L., and Hinton, G. 2008. Visualizing data using t-SNE. Journal of Machine Learning Research, 9: 2579–2605.

Vignon, M., and Morat, F. 2010. Environmental and genetic determinant of otolith shape revealed by a non-indigenous tropical fish. Marine Ecology Progress Series, 411: 231–241.

Volpedo, A. V., Tombari, A., and Echeverría, D. D. 2008. Eco-morphological patterns of the sagitta of Antarctic fish. Polar Biology, 31: 635–640.

Ward, R. D., Hanner, R., and Hebert, P. D. 2009. The campaign to DNA barcode all fishes, FISH-BOL. Journal of fish biology, 74: 329–356.

Wei, L., Zhu, G. P., and Yang, Q. Y. 2017. Length–weight relationships of five fish species associated with krill fishery in the Atlantic sector of the Southern Ocean. Journal of Applied Ichthyology, 33: 1303–1305.

Wei, X. Y., and Zhu, G. P. 2022. Shape and ontogenetic changes in otolith of the ocellated icefish (*Chionodraco rastrospinosus*) from the Bransfield Strait, Antarctic. Zoology, 153: 126025.

Wijayanto, U. W., and Sarno, R. 2018. An experimental study of supervised sentiment analysis using Gaussian Naïve Bayes. In 2018 International Seminar on Application for Technology of Information and Communication, pp. 476–481.

Williams, A., Koslow, J., Terauds, A., and Haskard, K. 2001. Feeding ecology of five fishes from the mid-slope micronekton community off southern Tasmania, Australia. Marine Biology, 139: 1177–1192.

Wong, J. Y., Chu, C., Chong, V. C., Dhillon, S. K., and Loh, K. H. 2016. Automated otolith image classification with multiple views: an evaluation on Sciaenidae. Journal of Fish Biology, 89: 1324–1344.

Yeung, H. W. F., Li, J., and Chung, Y. Y. 2017. Improved performance of face recognition using CNN with constrained triplet loss layer. In 2017 International Joint Conference on Neural Networks (IJCNN)pp. 1948–1955. IEEE.

Zhang, J., Lu, C., Wang, J., Yue, X. G., Lim, S. J., Al-Makhadmeh, Z., and Tolba, A. 2020. Training convolutional neural networks with multi-size images and triplet loss for remote sensing scene classification. Sensors, 20: 1188.

Zhu, G. P., Duan, M., Ashford, J. R., Wei, L., Zhou, M. X., and Bestley, S. 2018. Otolith nucleus chemistry distinguishes *Electrona antarctica* in the westward-flowing Antarctic Slope Current and eastward-flowing Antarctic Circumpolar Current off East Antarctica. Marine Environmental Research, 142: 7–20.

Handling Editor: Christopher Whidden

Received: 27 September 2022; **Revised:** 17 January 2023; **Accepted:** 10 March 2023